

## Linked-cluster series-expansion technique for quantum spin systems

Chris Wentworth and Yung-Li Wang

*Department of Physics, Florida State University, Tallahassee, Florida 32306*

(Received 11 August 1986; revised manuscript received 15 July 1987)

The linked-cluster series expansion is developed for use on models of quantum spin systems with single-ion potentials. A Wick-like theorem is used to calculate the  $\tau$  integrals occurring in the series expansion. Such a new approach can deal with many realistic models of magnetic materials and will yield high-accuracy results in both ordered and disordered phases. These developments are illustrated by calculating the first seven terms of the linked-cluster series for the free energy, susceptibility, specific heat, and spontaneous magnetization of the spin-1 anisotropic Heisenberg model with a uniaxial single-ion potential. Thermodynamic properties of the system in both paramagnetic and magnetically ordered phases are discussed including the magnetization and susceptibility as functions of temperature, the critical exponents  $\beta$  and  $\gamma$ , and the existence of tricritical and bicritical points.

### I. INTRODUCTION

In quantum statistical mechanics, diagrammatic Green's function and linked-cluster expansion methods have provided the most accurate results for many-body problems in boson and fermion systems. The methods have also been employed for treating the quantum spin systems.<sup>1</sup> Dramatic improvement of the results over the mean-field approximation is observed, however, the treatment has been confined to the simple models. For real magnetic materials, the crystal-field anisotropy plays a major role in many cases. The inclusion of the single-ion anisotropy in the Heisenberg model makes the many-body perturbation calculation much more difficult. Furthermore, the Green function and linked-cluster methods with high-density expansion ( $1/z$  expansion,  $z$  being the number of nearest-neighbor spins interacting with the spin), often yielded some unphysical results.<sup>2,3</sup>

At temperatures above the transition point, the high-temperature series-expansion method<sup>4</sup> has been used to treat the Heisenberg model (with anisotropic exchange interactions) and has obtained the most accurate critical temperature and critical exponents. Again, no high-order series has been obtained with the crystal-field anisotropy included.

In this paper a linked-cluster expansion method for models of quantum spin systems with crystal-field potentials is presented. The recently developed Wick reduction theorem<sup>5</sup> enables high-order series to be produced for the general quantum spin models. Instead of using the high-density approximation, the method sums up all perturbation terms to a certain order and estimates the results through well-developed extrapolation processes (the standard ratio method and the Padé approximants method). The perturbation used in this calculation is the part of the Hamiltonian which represents correlations of fluctuations of the spin variables ignored entirely in the mean-field approximation. The results of this calculation cover the whole range of temperature, both magnetically ordered and disordered phases. In the disordered

phase the results are identical to the high-temperature series. In the ordered phase, correlations of spin fluctuations from their thermal averaged values are included systematically in this perturbation expansion and yield results of high accuracy. The unphysical results produced by the high-density approximations are avoided in this approach.

The method developed here is based on the linked-cluster expansion<sup>6</sup> which has been used with success to form long series for classical systems. A twelfth-order high-temperature series for the spin-spin correlation function was obtained by this method for the Ising ferromagnet,<sup>7</sup> and a ninth-order high-temperature series was obtained for the classical anisotropic Heisenberg model.<sup>8</sup> Recently an eighth-order series expansion for the free energy in finite field of the Blume-Capel model<sup>9</sup> was obtained allowing the magnetization series to be calculated and first-order phase transitions to be discussed. This last calculation pointed out the usefulness of using the linked-cluster expansion to form a single series which covers both the ordered and disordered phases of a system.

Using the linked-cluster expansion to generate series for quantum spin systems is more problematic because of noncommutativity of the spin operators. High-temperature series expansions through fourth order have been obtained for models with Heisenberg exchange and single-ion potentials.<sup>10-12</sup> These calculations demonstrated how the single-ion potentials could be treated exactly using a linked-cluster series expansion methodology.

A modified Wick reduction theorem enabled a linked-cluster series expansion of tenth order in the paramagnetic phase and of eighth order in the ordered phase to be calculated for the transverse susceptibility of the Ising model<sup>5</sup> and the Blume-Capel model.<sup>13</sup> These calculations suggested a computational methodology which could be applied to Heisenberg exchange models with greater efficiency than the techniques used before.<sup>10-12</sup> The description of this methodology is the subject of this

paper.

The computational methodology presented here is appropriate for general spin and any single-ion potential which can be written in terms of spin operators, however for the sake of clarity the details are expressed in terms of a specific example model: the spin-1 anisotropic Heisenberg exchange model with a uniaxial single-ion anisotropy.

Section II will describe how the linked-cluster series expansion of the free energy for this model is obtained. The rules for writing down the terms in the expansion are described, and the use of the Wick theorem in evaluating  $\tau$  integrals is illustrated. The results of a sixth-order expansion are discussed in Sec. III where the use of standard extrapolation techniques to obtain properties over the entire temperature range is illustrated. A conclusion is given in Sec. IV.

## II. LINKED-CLUSTER SERIES EXPANSION AND THE WICK INTEGRAL FORMULA

The model Hamiltonian being considered is given by

$$H = - \sum_{i,j} J_{ij} (RS_i^+ S_j^- + S_i^z S_j^z) - \sum_i D (S_i^z)^2 - h \sum_i S_i^z. \quad (1)$$

$$\langle S(\beta) \rangle_0 = \sum_{n=0}^{\infty} (-1)^n / n! \int_0^\beta d\tau_1 \int_0^\beta d\tau_2 \cdots \int_0^\beta d\tau_n \langle T_\tau \{ H_1(\tau_1) H_1(\tau_2) \cdots H_1(\tau_n) \} \rangle_0. \quad (6)$$

Operators in Eq. (6) are written in the interaction picture, and  $T_\tau$  is the Dyson  $\tau$ -ordering operator which orders operators in the product with  $\tau$  labels decreasing from left to right.

The terms in Eq. (6) can be represented by bond graphs and when written in terms of semi-invariants allow the free energy to be expressed<sup>6</sup> as

$$\ln \langle S(\beta) \rangle_0 = \sum_{n, c_n} 1/n! W(c_n) L(c_n) V(c_n). \quad (7)$$

The summation is over all linked (connected) graphs where  $c_n$  indicates an  $n$ th-order linked graph.  $W(c_n)$  is the weight of the graph or the number of times the graph appears in the expansion.  $L(c_n)$  is the lattice constant of the graph.  $V(c_n)$  is the value of the  $\tau$  integral of the semi-invariant product which the graph represents. Table I lists all of the free-energy graphs through sixth order which contain longitudinal, or  $(S_i^z - M)(S_j^z - M)$ , interaction lines only. Table II lists all graphs through sixth order which contain transverse interaction lines.

The graphs in Table I, which contain longitudinal interaction lines only, have been used to calculate high-temperature series for the specific heat and the susceptibility for spin- $\frac{1}{2}$  and spin-1 Ising models. The series obtained from these graphs agree with previous results.<sup>15</sup>

The graphs in Table II, which contain transverse in-

teractions lines, are produced from the graphs of Table I by a simple algorithm which has been implemented on machine. An outline of this algorithm follows.

All transverse graphs will have an underlying topology of one of the pure longitudinal graphs, so one starts with a longitudinal graph with  $n$  lines. Call this graph  $c_{Ln}$ . Number the interaction lines of  $c_{Ln}$  from 1 to  $n$ . To generate diagrams with  $m$  transverse interaction lines do the following.

$$H = H_0 + H_1, \quad (2)$$

$$H_0 = \sum_i [ -(h + 2JzM) S_i^z - D (S_i^z)^2 + Jz M^2 ], \quad (3)$$

$$H_1 = - \sum_{i,j} J_{ij} [ R S_i^+ S_j^- + (S_i^z - M)(S_j^z - M) ]. \quad (4)$$

The parameter  $M$  is chosen to minimize the free energy. It can be shown that  $M$  is equal to the self-consistent value of the thermal average  $\langle S^z \rangle$ . The perturbation restores the effects of fluctuation correlations.

The free energy  $F$  can then be written in the form

$$-\beta F = -\beta F_0 + \ln \langle S(\beta) \rangle_0, \quad (5)$$

where  $\beta$  is the inverse of the temperature and  $F_0$  is the free-energy term corresponding to the unperturbed Hamiltonian  $H_0$ . The thermal average  $\langle S(\beta) \rangle_0$  in Eq. (5) is over the  $H_0$  ensemble and is expressed as<sup>14</sup>

(1) Choose, without regard to order,  $m$  lines from the  $n$  lines of  $c_{Ln}$ . This produces a list of graphs in which each graph has  $m$  specified transverse lines.

(2) For each graph in the list produced by step (1) assign directions to the transverse lines in all possible ways such that the numbers of heads and tails of lines at each vertex are equal to each other. This produces an expanded list of graphs.

(3) Search the list of graphs produced in step (2) to find classes of isomorphic graphs. Two graphs are isomorphic if they can be mapped into each other by switching vertices or lines without breaks. This produces a list of unique graphs each with an associated weight.

(4) Assign a final weight  $W(c_{Tm})$  to each unique graph produced in step (3) according to

$$W(c_{Tm}) = W(c_{Ln}) N_I(c_{Tm}) / 2^m. \quad (8)$$

TABLE I. List of free-energy graphs through sixth order which contain longitudinal bonds only. LC number labels the lattice constant.

Name	Weight	L.C.	Graph	Name	Weight	L.C.	Graph	Name	Weight	L.C.	Graph
D2001	2	201		D5007	960	506		D6012	5760	608	
D3001	4	301		D5009	384	507		D6013	5760	605	
D3002	8	302		D6001	32	601		D6014	5760	606	
D4001	8	401		D6002	960	602		D6015	23040	608	
D4002	48	402		D6003	640	602		D6017	11520	609	
D4003	96	403		D6004	960	604		D6018	5760	611	
D4004	48	404		D6005	960	603		D6019	2880	605	
D5001	16	501		D6006	3840	603		D6020	1920	613	
D5002	320	502		D6007	3840	606		D6021	11520	607	
D5003	320	503		D6008	11520	606		D6022	23040	610	
D5004	480	503		D6009	960	603		D6023	3840	612	
D5005	960	505		D6010	2880	604		D6026	3840	614	
D5006	960	504		D6011	3840	605					

$W(c_{Ln})$  is the weight of the original pure longitudinal graph  $c_{Ln}$ ;  $N_I(c_{Tm})$  is the number of isomorphic graphs in the list of step (2).

Graphs are represented by a matrix where each row corresponds to a vertex and each column corresponds to an interaction line. The result of applying a machine implementation of the above algorithm will be a file containing matrices and associated numbers for the weights and lattice constants.

The calculation proceeds by constructing all linked graphs up to a given order of the perturbation. The contribution of an  $n$ th-order graph to the free energy is given by the following rules.

(1) Associate a  $\tau$  label with each bond and a site label with each vertex.

(2) Associate  $J_{ij}$  with each bond.

(3) Associate a spin-operator product with each vertex where the operators are specified by the bonds ending on the vertex: a longitudinal bond contributes  $(S_i^z - M)$ , a transverse bond pointing into a vertex contributes  $S_i^-$ , and a transverse bond pointing out of the vertex contributes  $S_i^+$ . Assign the  $\tau$  label of each bond to the corresponding operators. Form the semi-invariant of the  $\tau$ -ordered product associated with each vertex.

(4) Form the product of semi-invariant and factors of  $J_{ij}$  associated with the graph.

(5) Integrate  $\tau$  variables from 0 to  $\beta$ .

(6) Sum the lattice labels over all lattice sites.

(7) Multiply the contribution by the weight of the graph.

(8) Divide the result by  $n!$ .

It should be noted that dividing the Hamiltonian in the way shown in Eqs. (2)–(4) and choosing the parameter  $M$  to be  $\langle S^z \rangle$  accomplishes a partial vertex renormalization which eliminates the single-tail graphs,<sup>16</sup> which have two parts connected by a single bond.

Summation over the lattice sites is achieved by choosing the appropriate free multiplicity<sup>6</sup> as the lattice constant and multiplying the term by  $(Jz)^n$ ,  $z$  being the number of nearest-neighbors interacting with a spin. The free multiplicities can be expressed in terms of weak embedded lattice constants used in the conventional high-temperature series expansion.<sup>17</sup> The relations between the two types of lattice constants are presented in Table III.

The major portion of the calculation is the evaluation of the  $\tau$  integrals implied by each graph. The multiple-site Wick reduction theorem discussed by Wang, Wentworth, and Westwanski<sup>5</sup> is employed to facilitate the calculation. The theorem applies to the thermal average of the ordinary (moment) product of  $\tau$ -ordered operators instead of the semi-invariant (cumulant) of a product, and the  $\tau$  dependence of each operator must be of the simple form

$$O(\tau) = e^{\epsilon\tau} O(0). \quad (9)$$

Therefore, the first step in the calculation of a  $\tau$  integral is to express the semi-invariants in terms of moments. This is done through the use of Eq. (10), where  $[S_1 S_2 \cdots S_n]_c$  represents the semi-invariant of the enclosed product of spin operators:

TABLE II. List of free-energy graphs through sixth order which contain transverse bonds.

Name	Weight	L.C.	Graph	Name	Weight	L.C.	Graph	Name	Weight	L.C.	Graph
D2201	1	201		D6602	180	602		D6216	2880	608	
D3201	6	301		D6204	1920	602		D6308	5760	608	
D3301	2	302		D6404	1440	602		D6413	720	608	
D4201	24	401		D6205	1440	604		D6609	360	608	
D4401	3	401		D6405	720	604		D6610	180	608	
D4202	48	402		D6603	120	604		D6217	5760	605	
D4402	12	402		D6206	2880	603		D6414	1440	605	
D4203	48	403		D6301	960	603		D6415	2880	605	
D4301	48	403		D6406	360	603		D6218	2880	606	
D4403	6	404		D6501	720	603		D6219	2880	606	
D5201	80	501		D6207	5760	603		D6309	2880	606	
D5401	30	501		D6208	1920	603		D6417	1440	606	
D5202	480	502		D6302	5760	603		D6508	1440	606	
D5203	160	502		D6407	2880	603		D6220	11520	608	
D5402	240	502		D6503	1440	603		D6310	11520	608	
D5204	480	503		D6209	5760	606		D6312	5760	608	
D5301	240	503		D6304	960	606		D6418	5760	608	
D5501	60	503		D6505	1440	606		D6509	2880	608	
D5205	480	503		D6210	5760	606		D6223	5760	609	
D5302	480	503		D6211	5760	606		D6421	1440	609	
D5403	120	503		D6305	5760	606		D6611	720	609	
D5206	480	505		D6408	2880	606		D6314	2880	611	
D5304	240	505		D6506	2880	606		D6612	360	611	
D5503	120	505		D6212	1440	603		D6224	2880	605	
D5207	480	504		D6307	1920	603		D6422	720	605	
D5404	240	504		D6409	720	603		D6423	1440	605	
D5305	480	506		D6604	120	603		D6315	1920	613	
D5405	120	506		D6605	30	603		D6425	720	613	
D5504	24	507		D6213	2880	604		D6225	5760	607	
D6201	240	601		D6214	1440	604		D6511	1440	607	
D6401	180	601		D6410	1440	604		D6316	5760	610	
D6601	10	601		D6411	720	604		D6426	2880	610	
D6202	2880	602		D6606	360	604		D6512	1440	610	
D6203	480	602		D6215	5760	605		D6427	1440	612	
D6402	360	602		D6412	1440	605		D6613	120	614	
D6403	1440	602		D6607	360	605					

$$[T\{S_1(\tau_1) \cdots S_n(\tau_n)\}]_c = \sum_{k=1}^n (k-1)!(-1)^{k-1} \sum_{p(n,k)} \left\langle T \left\{ \prod_{i=1}^{j_1} S_{a_{1i}}(\tau_{a_{1i}}) \right\} \right\rangle_0 \cdots \left\langle T \left\{ \prod_{i=1}^{j_k} S_{a_{ki}}(\tau_{a_{ki}}) \right\} \right\rangle_0, \quad (10)$$

$p(n,k)$  represents the set of partitions of  $n$  operators  $S_1, \dots, S_n$  into  $k$  sets without regard to order where  $j_1, \dots, j_k$  represent the number of operators in each set. The  $a_{ij}$  identifies operators within a set. Another useful property of semi-invariants is given by Eq. (11), where the  $c_i$  are constants and  $n > 1$ :

$$[T\{(S_1(\tau_1) - c_1) \cdots (S_n(\tau_n) - c_n)\}]_c = [T\{S_1(\tau_1) \cdots S_n(\tau_n)\}]_c. \quad (11)$$

Equation (12) gives an example of the use of Eqs. (10) and (11) in expressing the semi-invariants implied by graph D4202 (Table II) in terms of moments where  $p = \langle S^z \rangle_0$ :

$$\begin{aligned} & [T\{S_1^-(\tau_1)S_1^+(\tau_2)(S_1^z(\tau_3) - M)(S_1^z(\tau_4) - M)\}]_c [T\{S_2^+(\tau_1)S_2^-(\tau_2)\}]_c [T\{(S_3^z(\tau_3) - M)(S_3^z(\tau_4) - M)\}]_c \\ &= \langle T\{S_1^-(\tau_1)S_1^+(\tau_2)(S_1^z(\tau_3) - p)(S_1^z(\tau_4) - p)\} \rangle_0 \langle T\{S_2^+(\tau_1)S_2^-(\tau_2)\} \rangle_0 \langle T\{(S_3^z(\tau_3) - p)(S_3^z(\tau_4) - p)\} \rangle_0 \\ & - \langle T\{S_1^-(\tau_1)S_1^+(\tau_2)\} \rangle_0 \langle T\{S_2^+(\tau_1)S_2^-(\tau_2)\} \rangle_0 \langle T\{(S_1^z(\tau_3) - p)(S_1^z(\tau_4) - p)\} \rangle_0 \\ & \times \langle T\{(S_3^z(\tau_3) - p)(S_3^z(\tau_4) - p)\} \rangle_0. \end{aligned} \quad (12)$$

TABLE III. The free multiplicity lattice constants expressed in terms of weak embedded lattice constants.

LC number	LC in terms of weak embedded lattice constants
201	$z$
301	$z$
302	$6p_3$
401	$z$
402	$z^2$
403	$6p_3$
404	$8p_4 + 2z^2 - z$
501	$z$
502	$z^2$
503	$6p_3$
504	$8p_4 + 2z^2 - z$
505	$6zp_3$
506	$4p_{5A} + 6p_3$
507	$10p_{5A} + 30zp_3 - 30p_3$
601	$z$
602	$z^2$
603	$6p_3$
604	$z^3$
605	$8p_4 + 2z^2 - z$
606	$6zp_3$
607	$10p_5 + 30zp_3 - 30p_3$
608	$4p_{5A} + 6p_3$
609	$8zp_4 + 2z^3 - z^2$
610	$2p_{6B} + 8p_{5A} + 12zp_3 - 6p_3$
611	$36p_3^2$
612	$12p_{6A} + 24p_4 + z^3 + z^2 - z$
613	$24p_{6D}$
614	$12p_6 + 24p_{6C} + 12p_{5A} - 48p_4 + 48p_4z + 6p_3 + 2z - 6z^2 + 5z^3$

A program has been developed which allows this algebra to be done by machine.

After semi-invariants have been expressed in terms of moments, then the spin operators in each product are represented in terms of standard basis operators created based on the unperturbed Hamiltonian  $H_0$ . The eigenstates of  $H_0$  for the spin-1 system considered here are the same as those of the operators  $S^z$ , and the eigenenergies are given in Eqs. (13)–(15):

$$E_1 = -D - h - 2Jz \langle S^z \rangle + \langle S^z \rangle^2 Jz, \quad (13)$$

$$E_0 = \langle S^z \rangle^2 Jz, \quad (14)$$

$$E_{-1} = -D + h + 2Jz \langle S^z \rangle + \langle S^z \rangle^2 Jz. \quad (15)$$

If  $|k, 1\rangle$ ,  $|k, 0\rangle$ , and  $|k, -1\rangle$  are the corresponding eigenstates for site  $k$  then the standard basis operators are defined as

$$L_{ij}^k = |k, i\rangle \langle k, j|. \quad (16)$$

Standard basis operators for different sites commute while those having the same site satisfy

$$[L_{ij}, L_{kl}] = L_{il} \delta_{jk} - L_{kj} \delta_{li}. \quad (17)$$

The standard basis operators in the interaction picture have the simple  $\tau$  dependence which the Wick reduction theorem requires as Eq. (18) demonstrates:

$$L_{ij}(\tau) = \exp[(E_i - E_j)\tau] L_{ij}. \quad (18)$$

The spin operators are written in terms of the standard basis operators in Eqs. (19)–(21):

$$S^+ = \sqrt{2}(L_{10} + L_{0-1}), \quad (19)$$

$$S^- = \sqrt{2}(L_{01} + L_{-10}), \quad (20)$$

$$S^z = L_{11} - L_{-1-1}. \quad (21)$$

The replacement of spin operators by standard basis operators is done with a simple algorithm which has been implemented on machine. First, sums of standard basis operator products which can give rise to nonzero contributions are developed for each product of spin operators. For a standard basis operator product to give a nonzero contribution it is necessary for every raising operator,  $L_{10}$  and  $L_{0-1}$ , to be matched in the product by a lowering operator,  $L_{01}$  or  $L_{-10}$ . These lists are regarded as data for a symbolic multiplying program. For each spin-operator graph this program does the following.

(1) The spin-operator products associated with each vertex are replaced by corresponding sums of standard basis operator products.

(2) The product of sums produced in step (1) are multiplied out.

(3) To aid in summing equivalent terms, the thermal averages in each product are commuted so that

equivalent thermal averages appear in the same order when they occur in different terms.

(4) The rearranged sum from step (3) is inspected for equivalent terms which are summed together.

Once the spin operators in an integrand have been expressed in terms of standard basis operators then all operators with the same  $\tau$  are grouped together. The integrands is written in terms of the operator  $O_l$  defined as

$$\begin{aligned} O_l(\tau_l) &= O(i, j, \dots; ab, cd, \dots; \tau_l) \\ &= L_{ab}^i(\tau_l) L_{cd}^j(\tau_l) \cdots \end{aligned} \quad (22)$$

The original integral containing a product of spin operators will now be a sum of integrals containing products of the  $O$  operators defined in Eq. (22). Some of these integrals have  $\tau$ -independent integrands. They are calculated by forming all permutations of  $O$  operators, calculating the thermal average for each permutation, and multiplying the sum of all permutations by  $\beta^n/n!$ . The integrals with  $\tau$ -dependent integrands are calculated by using the Wick reduction theorem<sup>5</sup> of Eq. (23):

$$\begin{aligned} &\int_0^\beta d\tau_1 \cdots \int_0^\beta d\tau_k \cdots \int_0^\beta d\tau_n \langle T\{O_1(\tau_1) \cdots O_k(\tau_k) \cdots O_n(\tau_n)\} \rangle_0 \\ &= \frac{1}{\epsilon_k} \int_0^\beta d\tau_1 \cdots \int_0^\beta d\tau_n (\langle T\{[O_1, O_k]_{\tau_1} \cdots O_n(\tau_n)\} \rangle_0 + \cdots + \langle T\{O_1(\tau_1) \cdots [O_n, O_k]_{\tau_n}\} \rangle_0), \end{aligned} \quad (23)$$

$$\epsilon_k = (E_{a_k} - E_{b_k}) + (E_{c_k} - E_{d_k}) + \cdots, \quad (24)$$

$$[O_i, O_j]_{\tau_i} = [O_i(\tau_i), O_j(\tau_i)]. \quad (25)$$

Use of Eq. (23) expresses an  $n$ th-order integral as a sum of  $(n-1)$ th-order integrals. Equation (23) or the  $\tau$ -independent procedure can be applied to each integral in the sum until all integrations have been completed. The  $(n-1)$ th-order integrals appearing in Eq. (23) could have been calculated when lower-order terms were considered. If their values have been catalogued then the integration procedure just described can be abbreviated.

The Wick integration procedure is demonstrated on an integral given in Eq. (26) which is generated from the third-order ring graph with all transverse interaction lines,

$$I_r = \int_0^\beta d\tau_1 \int_0^\beta d\tau_2 \int_0^\beta d\tau_3 \langle T\{L_{10}^1(\tau_1) L_{01}^1(\tau_2)\} \rangle_0 \langle T\{L_{0-1}^2(\tau_2) L_{-10}^2(\tau_3)\} \rangle_0 \langle T\{L_{-10}^3(\tau_1) L_{0-1}^3(\tau_3)\} \rangle_0. \quad (26)$$

Operators with the same  $\tau$  are grouped together;

$$I_r = \int d\tau_1 \int d\tau_2 \int d\tau_3 \langle T\{O(1, 3; 10, -10; \tau_1) O(1, 2; 01, 0-1; \tau_2) O(2, 3; -10, 0-1; \tau_3)\} \rangle_0. \quad (27)$$

The first operator in the product of Eq. (27) is chosen to be  $O_k$  in Eq. (23). Application of the Wick integral formula gives

$$\begin{aligned} I_r &= -1/(2D)(\langle L_{00} \rangle_0 - \langle L_{11} \rangle_0) \int d\tau_2 \int d\tau_3 \langle T\{O(2, 3; 0-1, -10; \tau_2) O(2, 3; -10, 0-1; \tau_3)\} \rangle_0 \\ &\quad - 1/(2D)(\langle L_{00} \rangle_0 - \langle L_{-1-1} \rangle_0) \int d\tau_2 \int d\tau_3 \langle T\{O(1, 2; 01, 0-1; \tau_2) O(1, 2; 10, -10; \tau_3)\} \rangle_0. \end{aligned} \quad (28)$$

The first integral in Eq. (28) is  $\tau$  independent and can be calculated by the method for  $\tau$ -independent integrands described earlier. The second integral can be calculated by applying Eq. (23), again yielding a trivial one-dimensional integral. Both integrals would have been calculated when second-order terms were considered, so their values could be retrieved from a catalogue. The value of  $I_r$  is given by

$$\begin{aligned} I_r &= \beta^3/(2\beta D) \langle L_{00} \rangle_0 \langle L_{-1-1} \rangle_0 (\langle L_{-1-1} \rangle_0 - \langle L_{00} \rangle_0) \\ &\quad + \beta^3/(2\beta D)^2 (\langle L_{11} \rangle_0 \langle L_{-1-1} \rangle_0 - \langle L_{00} \rangle_0^2) \\ &\quad \times (\langle L_{-1-1} \rangle_0 - \langle L_{00} \rangle_0). \end{aligned} \quad (29)$$

The thermal average of a standard basis operator can be calculated easily. Equations (30)–(32) give the averages

for the model under consideration:

$$\langle L_{11} \rangle_0 = \frac{1}{2}(q+p), \quad (30)$$

$$\langle L_{00} \rangle_0 = 1-q, \quad (31)$$

$$\langle L_{-1-1} \rangle_0 = \frac{1}{2}(q-p), \quad (32)$$

$$p = \exp(\beta D) [\exp(\beta h_e) - \exp(-\beta h_e)] / Z_0, \quad (33)$$

$$q = \exp(\beta D) [\exp(\beta h_e) + \exp(-\beta h_e)] / Z_0, \quad (34)$$

$$Z_0 = 1 + \exp(\beta D) [\exp(\beta h_e) + \exp(-\beta h_e)], \quad (35)$$

$$h_e = h + 2JzM. \quad (36)$$

Use of the standard basis operators simplifies the algebra involved in calculating the  $\tau$  integrals, however it requires that a much larger number of integrals be considered. The simplicity of the algebra allows the integration procedure to be done by machine. A computer program has been developed which can evaluate a standard basis operator integral by the  $\tau$ -independent procedure, if applicable, or by successive application of the Wick reduction integral formula. Calculating and summing all standard basis operator integrals associated with the free-energy graphs through sixth order took approximately 19 h of computer time with about 75% of this done on a CDC Cyber 730 machine and about 25% done on a CDC Cyber 760 machine.

The free-energy series calculated in the manner described above takes the form of

$$-\beta F = -\beta F_0 + \sum_{n=2}^{\infty} f_n(x,y)(\beta J)^n, \quad (37)$$

where

$$x = \beta D, \quad (38)$$

$$y = \beta(h + 2JzM). \quad (39)$$

The coefficients  $f_n(x,y)$  are in the form of polynomials in  $p, q, R$ , and  $(\beta D)^{-1}$ . The other equilibrium thermodynamic properties can be obtained from Eq. (37) by differentiation. This algebra is done with the general symbol manipulation program SCHOONSCHIP.<sup>18</sup> The properties considered in this paper are the magnetization, susceptibility, and specific heat. The magnetization is given as

$$M = -\partial F / \partial h = -\partial(\beta F) / \partial y = p + \sum_{n=2}^{\infty} m_n(x,y)(\beta J)^n. \quad (40)$$

The susceptibility is calculated from Eq. (42) after forming the series for  $\beta^{-1}\chi_c$  defined in Eq. (41):

$$\beta^{-1}\chi_c = \partial M / \partial y, \quad (41)$$

$$\begin{aligned} \beta^{-1}\chi &= \beta^{-1}\chi_c / [1 - 2\beta Jz\beta^{-1}\chi_c] \\ &= q - p^2 + \sum_{n=1}^{\infty} a_n(x,y)(\beta J)^n. \end{aligned} \quad (42)$$

The specific-heat series is defined as

$$\begin{aligned} c_h k_B^{-1} &= x^2 \partial(-\beta F) / \partial x^2 \\ &= x^2(q - q^2) + \sum_{n=2}^{\infty} g_n(x,y)(\beta J)^n. \end{aligned} \quad (43)$$

The coefficients  $m_n, a_n$ , and  $g_n$  are expressed as polynomials in the variables  $(\beta D)^{-1}, p, q$ , and  $R$ . The coefficients with  $n$  equal to 1–6 have been obtained for a general lattice. In the appendix we list the polynomials of  $m_n$  and those of  $a_n$  and  $g_n$  in the paramagnetic phase for the fcc lattice. The coefficients  $a_n$  and  $g_n$  in the ordered phase are too long to be presented here. We refer the interested reader to Ref. 19.

Several checks have been performed to assess the validity of the series calculated in this investigation.

First of all, the result of the current calculation in the paramagnetic phase ( $T > T_c$ ), which is a high-temperature series expansion with general lattice constants, agree completely with that of Wang and Lee<sup>10</sup> who used the Green's function method to obtain the high-temperature series for the susceptibility of the same model up to the fourth order.

As a check on the completeness of the list of longitudinal graphs, Table I has been used to calculate high-temperature series expansions of the free energy and susceptibility for the spin- $\frac{1}{2}$  and spin-1 Ising models, and the results agree with previous results.<sup>15</sup>

The completeness of Table II has been checked by using it, together with Table I, to calculate high-temperature series for the spin- $\frac{1}{2}$  Heisenberg model with anisotropic exchange interactions. The value of a graph with transverse bonds was obtained by expressing cumulants in terms of moments (by machine) and calculating the value of each term by constructing all permutations of the  $\tau$  label and calculating the thermal average of each resulting operator product. The sixth-order zero-field free-energy series produced in this way agrees with that of Wood and Dalton,<sup>20</sup> and the susceptibility series agrees with that of Jou and Chen,<sup>21</sup> who calculated high-temperature susceptibility series for the spin- $\frac{1}{2}$  model and found some discrepancies with the Wood and Dalton series. This calculation suggests that Table II is correct and that the program which expresses cumulants in terms of moments contains no errors.

A second check on Table II and a check on the program, which expresses spin-operator terms as sums of standard basis operator terms, has been done by using the resulting sums to calculate the high-temperature series for the spin-1 anisotropic Heisenberg model without the single-ion anisotropy ( $D=0$ ). The results have been compared with those of Wood and Dalton.<sup>20</sup> The two series for the zero-field free-energy agree, however, there are discrepancies for the high-temperature susceptibility series. Equation (44) shows the high-temperature susceptibility series for the fcc lattice obtained in the present investigation:

$$a_1 = 10.66667, \quad (44a)$$

$$a_2 = 160 - 8.88889R^2, \quad (44b)$$

$$a_3 = 2339.5556 - 272.59259R^2 - 37.92592R^3, \quad (44c)$$

$$a_4 = 33\,691.259\,26 - 5899.061\,73R^2 - 1147.259\,26R^3 - 180.740\,74R^4, \quad (44d)$$

$$a_5 = 480\,371.2 - 111\,807.736\,62R^2 - 24\,358.452\,67R^3 - 3646.946\,50R^4 - 1536.526\,75R^5, \quad (44e)$$

$$a_6 = 6\,802\,245.794\,24 - 1\,972\,128.763\,79R^2 - 455\,265.272\,98R^3 - 39\,268.433\,47R^4 - 30\,430.990\,40R^5 - 13\,960.384\,09R^6. \quad (44f)$$

The published Wood and Dalton series<sup>20</sup> yields the same coefficients for  $a_0$  through  $a_4$ , however  $a_5$  and  $a_6$  show some differences. The Wood and Dalton coefficients  $a_5$  and  $a_6$  are shown as

$$a_5^{\text{WD}} = 480\,371.2 - 111\,953.119\,34R^2 - 24\,347.074\,90R^3 - 3512.941\,56R^4 - 1536.526\,75R^5, \quad (45a)$$

$$a_6^{\text{WD}} = 6\,802\,245.794\,24 - 1\,972\,221.471\,61R^2 - 455\,172.565\,16R^3 - 39\,453.849\,11R^4 - 30\,245.574\,76R^5 - 13\,960.384\,09R^6. \quad (45b)$$

Both results for the susceptibility series, Eqs. (44) and (45), agree with the isotropic Heisenberg series ( $R = 1$ )<sup>4</sup> and the Ising series ( $R = 0$ ).

Since the free energy calculated from Tables I and II agrees with the zero-field free-energy series of Wood and Dalton,<sup>20</sup> it suggests that these tables and the standard basis diagram lists are complete. In this investigation the susceptibility is formed by differentiation of the free energy, whereas the Wood and Dalton method requires a new set of graphs to calculate their susceptibility series. In calculating  $\chi$  the linked-cluster graphs generate contributions which are nonzero for all (nonzero) values of  $R$ , whereas the method used by Wood and Dalton generates certain graphs which become zero in the isotropic Heisenberg case. If the symbolic differentiation program used here does not introduce spurious exponents of  $R$  then the agreement of the current calculated series with the isotropic Heisenberg series<sup>4</sup> should be a strong indication of the correctness of the series in the case of anisotropic exchange interactions. The differentiation program has been checked by replacing  $R$  by a number at the beginning and comparing the resulting series for  $\chi$  with that obtained when  $R$  is left as a symbol. Agreement is found.

A more reliable and convincing way to distinguish the correct one of these two susceptibility series is to use an independent approach to derive the series. The finite-cluster method is a well-developed method for finding the high-temperature series for classical spin and certain quantum spin systems.<sup>4</sup> The method has been used by Jou and Chen<sup>21</sup> for deriving the susceptibility series to the seventh order for spin- $\frac{1}{2}$  Heisenberg model with anisotropic exchange interactions. For the spin-1 anisotropic Heisenberg model the calculation is more complicated because the size of the matrices is much larger. (For  $n$ -point clusters matrices are of order  $3^n$  as com-

pared with order  $2^n$  for the spin- $\frac{1}{2}$  case.) Instead of deriving the full series to the sixth order using the finite-cluster method we decided to make a partial check of the correctness of the Wood and Dalton series and the present series by comparing both results in a special case ( $z = 1$  and all  $p_{nx} = 0$ ) with the result of the two-point (connected) cluster in the finite-cluster method. By putting  $z = 1$  and all  $p_{nx} = 0$ , all clusters except the two-point cluster will yield zero contribution to the series.

To calculate the free energy and susceptibility of the two-point cluster, the  $9 \times 9$  matrix of the Hamiltonian, Eq. (1) with only two sites, can be reduced to one  $3 \times 3$ , two  $2 \times 2$ , and two  $1 \times 1$  matrices. The eigenenergies of the two-site Hamiltonian can be easily obtained and the partition function, free energy, and susceptibility can be calculated. The results of this finite-cluster calculation of the susceptibility series agree with that of Wood and Dalton (with  $z = 1$  and  $p_{nx} = 0$ ) except that there are differences in the fifth-order terms. The results of the series derived in this paper (with  $z = 1$  and  $p_{nx} = 0$ ) agree fully with the two-point finite-cluster results. The fifth-order term of the susceptibility series obtained by the two-point cluster calculation and the present linked-cluster expansion calculation with  $z = 1$  and  $p_{nx} = 0$  is shown as

$$a_5 = 112/3645 + 848/729R^2 + 512/729R^4. \quad (46a)$$

The result of the Wood and Dalton series is given by

$$a_5^{\text{WD}} = 112/3645 + 464/729R^2 + 896/729R^4. \quad (46b)$$

Only in the two particular cases (as mentioned above), Ising model ( $R = 0$ ) and isotropic Heisenberg model ( $R = 1$ ), the results of Wood and Dalton agree with the correct answer. Clearly, the two-point cluster calculation of the finite-cluster method provides a strong support of the correctness of the series obtained in this paper.

The Wick reduction integration program was checked with human calculation of selected standard basis operator terms at each order. As an additional test, the  $D$  equal to zero limit of the value of each spin-operator free-energy graph was taken and compared with the value obtained in the spin-1 anisotropic Heisenberg model calculation mentioned previously. Agreement was found for every graph; also, all singular  $(\beta D)^{-n}$  terms are observed to cancel in the  $D$  equal to zero limit.

The algebra required to go from Eq. (41) to (42) was done by machine. The final susceptibility series has been checked in the paramagnetic phase by taking the  $D$  equal to zero limit. The resulting series at  $D$  equal to zero agrees with the spin-1 anisotropic Heisenberg model series of Eq. (44).

The checks summarized here cannot guarantee with complete certainty that no errors were made in calculating the series expansions presented, however they do give strong confidence in the results.

### III. ANALYSIS OF THE SERIES AND DISCUSSION OF THE RESULTS

The mean-field picture of the spin-1 ferromagnetic Heisenberg model with anisotropic exchange interactions



and  $D(S^z)^2$  single ion potential has been given by Khajepour, Wang, and Kromhout.<sup>22</sup> Their analysis indicates that two kinds of ordered phases can be expected in zero field depending on the magnitudes of the exchange anisotropy  $R$  and the single-ion anisotropy  $D$ . The two kinds of ordering are a phase with longitudinal ( $Z$ ) ordering and a phase with transverse ( $XY$ ) ordering. If the exchange anisotropy  $R$  is greater than a certain critical value (equal to 0.462 in the mean-field approximation) then the  $D$ - $T$  phase diagram will display a bicritical point where two second-order lines merge with a first-order line. If  $R$  falls below this value then the phase diagram will display a tricritical point where a second-order line merges with a first-order line.

The series expansions presented here can be used to obtain information on the transition between longitudinally ordered ( $Z$ ) phase and the paramagnetic phase.

The second-order phase boundary in the  $D$ - $T$  plane between the longitudinal and paramagnetic phases can be obtained by looking at the divergence of the paramagnetic susceptibility series using the ratio method.<sup>23</sup> In the paramagnetic phase  $\chi$  is zero and  $\beta D$  can be fixed so that the phase boundary is approached on a path of constant slope in the  $D$ - $T$  plane. For each value of  $\beta D$ ,  $kT_c/J$  is estimated from

$$kT_{cn}/J = nr_n - (n-1)r_{n-1}. \quad (47)$$

In this equation,  $r_n = a_n/a_{n-1}$ . The associated value of  $D/J$  is obtained from the fixed value of  $\beta D$ . Figure 1 shows the second-order phase boundary in the  $D$ - $T$  plane for easy-axis values of  $D$  and for  $R = 0.25, 0.8$ , and 1 (isotropic Heisenberg exchange). The phase boundary for  $R = 0$  which corresponds to the Blume-Capel model is too close to that of  $R = 0.25$  to be plotted in this figure. For  $D = 0$  the model reduces to the spin-1 anisotropic Heisenberg exchange model, and for  $D$  approaching positive infinity the (longitudinal) properties of the model approach those of the spin- $\frac{1}{2}$  Ising exchange model. This asymptotic behavior follows from observing that the  $S^z = 0$  state is separated from the  $S^z = \pm 1$  states by an energy gap of  $D$ , due to the single-ion anisotropy.

In general, the uncertainty in the estimated values of

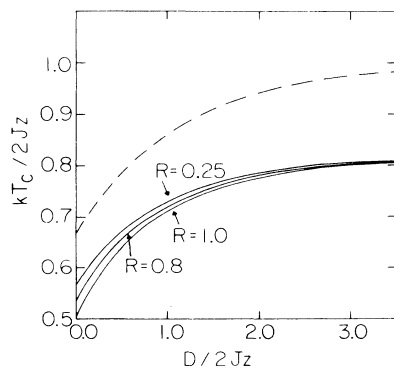


FIG. 1. Second-order phase boundary for easy-axis values of  $D$ .  $R = 0.25, 0.8$ , and 1.0; fcc lattice. Dashed line gives mean-field values. Solid line gives results of sixth-order series.

$kT_c/J$  increases for high values of  $R$  and lower values of  $D$ . For example, when  $R = 0.25$  and  $D/2Jz = 0.12$  the extrapolations for  $kT_c/J$  using second-, third-, fourth-, fifth-, and sixth-order series are 0.6116, 0.6060, 0.6018, 0.5999, and 0.5994; when  $R = 0.25$  and  $D/2Jz = 1.2$  then the corresponding extrapolations are 0.7627, 0.7510, 0.7483, 0.7472, and 0.7472. When  $R = 1$  and  $D/2Jz = 0.11$  the extrapolations are 0.5525, 0.5399, 0.5405, 0.5424, and 0.5443; when  $D/2Jz = 1.25$  the extrapolations are 0.7425, 0.7349, 0.7367, 0.7375, and 0.7381. If an uncertainty is assigned to these transition temperatures by taking the difference between the sixth-order and fifth-order extrapolations then it is always less than 0.002 and usually less than 0.001.

The mean-field phase boundary from the  $Z$  phase to the paramagnetic phase will show no variation with  $R$  since the effect of transverse exchange interaction enters into the mean-field approximation only when there is a moment in the transverse direction. The phase boundary is shown in the dashed line in Fig. 1 for comparison.

The variation of  $T_c$  with  $R$  which the series expansion predicts is shown more clearly in Fig. 2. The effects of the transverse exchange interaction enter through the perturbation and favor ordering in the transverse direction, so the transition temperature is expected to decline with increasing  $R$  as Fig. 2 indicates. The difference between  $T_c$  at  $R = 0$  and  $R = 1$  diminishes as  $D$  becomes large simply because the energy gap between the  $S^z = 0$  state and  $S^z = \pm 1$  states increases and the effect of the transverse coupling is weakened.

The magnetization as a function of temperature can be estimated using the ratio method. The series in  $\beta J$  for  $S/(M-S)$  is considered where  $S$  is the series of Eq. (33).  $S$  is a function of  $M$  so that if the correct pair  $(M, kT/2Jz)$  is used in  $S/(M-S)$  this function should diverge as the order of the series  $S$  goes to infinity. This suggests an iterative procedure for finding  $(M, kT/2Jz)$ . Fix  $D/J$ ,  $x$ , and  $y$ . Calculate the series coefficients. Es-

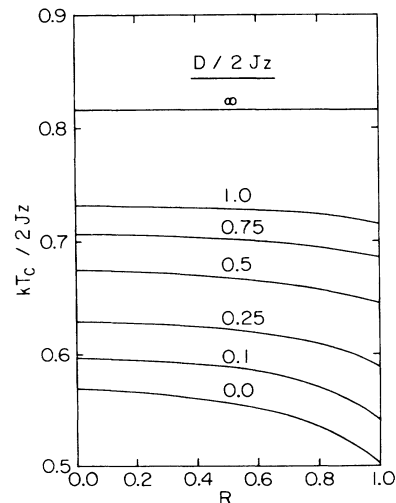


FIG. 2. Second-order transition temperatures as functions of  $R$  for easy-axis values of  $D$ . Results of sixth-order series; fcc lattice.

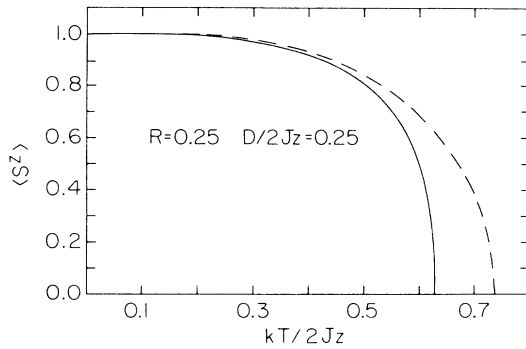


FIG. 3. Magnetization as a function of temperature.  $D/2Jz = 0.25$ .  $R = 0.25$ ; fcc lattice. Dashed line gives mean-field values. Solid line gives results of sixth-order series.

estimate the  $\beta J$  at which the series diverges. Compare with the  $\beta J$  calculated from  $x$ . Change  $x$  and repeat the procedure until self-consistency is achieved. Calculate  $M$  from  $y$  and  $\beta J$ . Carrying out this procedure for different  $y$  will give the  $M$ - $T$  curve.

Figures 3 and 4 show  $M$  as a function of  $T$  for easy axis and easy plane values of  $D$  and for  $R$  equal to 0.25. The easy-axis case shows good convergence over the entire temperature range. If an uncertainty is assigned to the magnetization by taking the difference between the sixth- and fifth-order extrapolations then it is always less than about 0.002.

The easy-plane result shows a spurious low-temperature feature (indicated by the dotted line in Fig. 4) which is due to using the ratio method to estimate the singularity in the function. The ratio method picks up the singularity on the real axis closest to the origin. If that singularity is not the physical one or if there are several nearby singularities then using the ratio method may not yield the correct extrapolations. A better estimate of the magnetization in the region surrounding  $kT/2Jz = 0.1$  can be obtained by looking at Padé approximants<sup>24</sup> to  $S/(M - S)$ . The coefficients of  $S$  and  $S/(M - S)$  are calculated by choosing trial values of  $M$

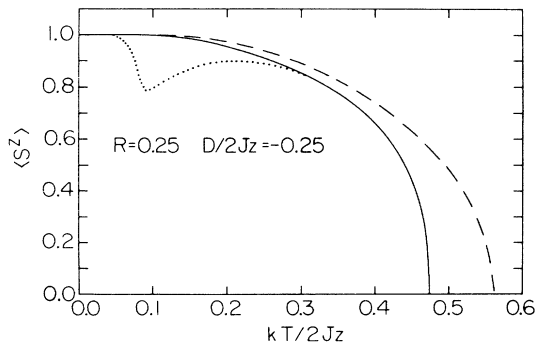


FIG. 4. Magnetization as a function of temperature.  $D/2Jz = -0.25$ .  $R = 0.25$ ; fcc lattice. Dashed line gives mean-field values. Solid line gives results of sixth-order series. Dotted line shows the spurious result of using the ratio method extrapolation.

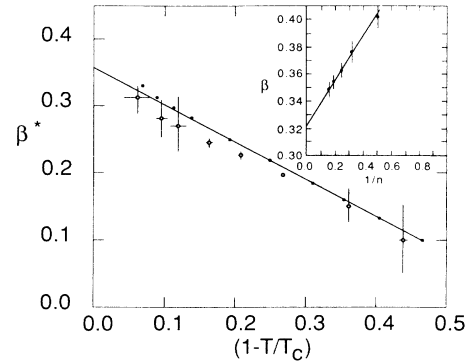


FIG. 5. The solid circles show  $\beta^*$  vs  $(1 - T/T_c)$  for  $D/2Jz = 1.027$  and  $R = 0.25$  calculated from the sixth-order series expansion for the fcc lattice. The inset shows the estimates of  $\beta$  for each order and the extrapolation to infinite order. The open points show results for the Ising model calculated by Gaunt and Baker (Ref. 25).

and  $\beta J$ ; Padé approximants to  $S/(M - S)$  are calculated; the roots of the denominator are found; these roots provide estimates of  $\beta J$  from which the corresponding  $M$  is calculated. The procedure is repeated with the new estimate of  $M$  until self-consistency is achieved. Estimates made in this way yield the low-temperature portion of the curve in Fig. 4 where the uncertainty in  $\langle S^z \rangle$  is now comparable to that of the easy-axis case.

An estimate for the critical exponent  $\beta$  associated with the magnetization can be obtained by making a plot of  $\ln M$  versus  $\ln(1 - T/T_c)$ . Estimating  $\beta$  in this way yields a range of values between 0.26 and 0.40. A more precise method of estimating  $\beta$  is to follow Gaunt and Baker<sup>25</sup> and plot  $\beta^*$  versus  $(1 - T/T_c)$  where  $\beta^*$  is given by

$$\beta^* = -(kT_c/J)(1 - T/T_c)(1/M)\partial M/\partial(kT/J). \quad (48)$$

Figure 5 shows an example of such a plot for

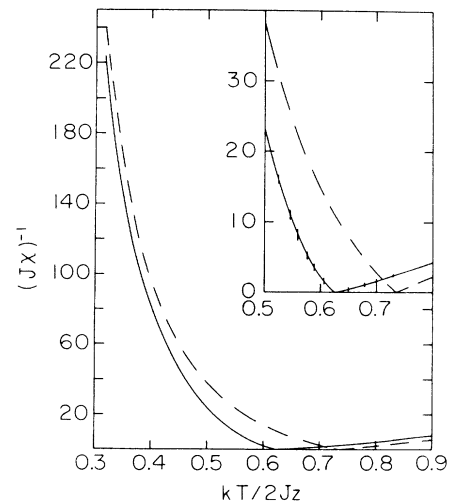


FIG. 6. Susceptibility as a function of temperature.  $D/2Jz = 0.25$ .  $R = 0.25$ ; fcc lattice. Dashed line gives the mean-field values. Solid line gives results of sixth-order series.

TABLE IV. Neville table for  $\gamma^{(n)}$ .  $D/2Jz = 0.2515$  and  $R = 0.25$ .

$m/n$	1	2	3	4	5
0	1.168	1.190	1.210	1.222	1.225
1		1.213	1.249	1.258	1.241
2			1.267	1.266	1.216

$D/2Jz = 1.0273$  and  $R = 0.25$  using the sixth-order series expansion for the magnetization. The intercept with the  $\beta^*$  axis of the linear fit for these points is taken to be the sixth-order estimate for  $\beta$ . The inset of Fig. 5 shows the estimates for  $\beta$  using second-, third-, fourth-, fifth-, and sixth-order series plotted against  $1/n$  where  $n$  is the order. Extrapolating to  $1/n$  equal to zero gives  $\beta = 0.32 \pm 0.1$ . Values for  $\beta^*$  calculated from Eq. (48) show large deviations from linearity for  $(1 - T/T_c) < 0.15$ , so points in the temperature range  $0.15 < (1 - T/T_c) < 0.45$  were used to form a best-fit line. A major source of uncertainty in each estimate of  $\beta$  is the uncertainty in  $T_c$ . This uncertainty is indicated in Fig. 5, and from this an uncertainty of about 0.01 in the extrapolated  $\beta$  is obtained. Data from the twelfth-order Ising model series for a bcc lattice which Gaunt and Baker analyzed is presented in Fig. 5 for comparison.

Estimates of the susceptibility as a function of temperature can be obtained by looking at the Padé approximants to the series. Figure 6 shows an example of  $\chi^{-1}$  versus temperature for an easy-axis value of  $D$  where  $\chi^{-1}$  was estimated from the average of the  $[\frac{3}{3}]$  and  $[\frac{2}{4}]$  approximants and the uncertainty is estimated from the difference between the  $[\frac{3}{3}]$  and  $[\frac{2}{3}]$  approximants. This curve shows Curie law behavior at high temperatures with deviations beginning at approximately  $T = 1.15T_c$ . It also shows the temperature behavior of the susceptibility in the ordered phase.

The exponent  $\gamma$  can be estimated from the series with higher accuracy on the paramagnetic side. The ratio method is used in such an estimation with values of  $D$  and  $R$  fixed.

$$\gamma^{(n)} = 1 + n \{ r_n / [nr_n - (n-1)r_{n-1}] - 1 \}. \quad (49)$$

It is noticed that in many cases  $\gamma^{(n)}$  still increases mono-

tonically instead of reaching a final value in the present analysis. Constructing a Neville table for  $\gamma$  shows significant improvement in estimating the final value of  $\gamma$ . As an example, the Neville table of  $\gamma$  for  $D = 0.2515$  and  $R = 0.25$  is shown in Table IV. The Neville table estimates  $I_n^m$  are constructed using

$$I_n^m = [nI_n^{m-1} - (n-m)I_{n-1}^{m-1}] / m, \quad (50)$$

where

$$I_n^0 = \gamma^{(n+1)}. \quad (51)$$

The procedure for estimating  $\gamma$  was to average  $I_n^m$  for  $n$  equal to 3, 4, and 5 for the  $m$  which shows the best convergence. The uncertainty was taken to be the largest difference between the average and each  $I_n^m$  used in calculating the average. The exponent  $\gamma$  can be estimated with high accuracy for positive, easy-axis values of  $D$ . The value is  $1.25 \pm 0.01$  for all values of  $D$ . Another limit where the estimate of  $\gamma$  shows high accuracy is when  $D/2Jz$  reaches its tricritical value of  $-0.466$  where  $\gamma = 1.00 \pm 0.01$ . As is shown in Table V, the values of  $\gamma$  changes gradually from its critical value to the tricritical value as  $D$  approaches  $D_t$ , and the tricritical value dominates in the neighborhood of  $D_t$ . This is usual behavior observed in the series analysis of other models.<sup>26</sup>

For systems with easy-plane single-ion anisotropy ( $D < 0$ ), a first-order phase transition may occur as mentioned above. For  $R$  smaller than a critical value  $R_c$  the phase diagram in the  $(D, T)$  plane exhibits a tricritical point where the nature of the phase transition changes from second order (continuous) to first order (discontinuous). To locate the tricritical point we use the magnetization series to estimate  $\langle S^z \rangle$  as a function of temperature for a fixed value of  $D$ . If the phase transition is first order  $\langle S^z \rangle$  becomes multivalued at temperatures close to the transition point. The tricritical point can then be estimated through the observation of the behavior of  $\langle S^z \rangle$ . In Fig. 7, for various values of  $R$  we show lines of divergent susceptibility. The second-order phase boundary ends at the tricritical point marked by an open circle. Beyond the tricritical point the curve continues as a spinodal line. The  $R = 0$  curve and the tricritical point location are in good agreement with the results of the eighth-order linked-cluster series analysis of the Blume-Capel model by Wang and Lee.<sup>9</sup> The uncertainty in the location of the tricritical points was estimated from the difference between the sixth-order estimate and the fifth-order estimate.

As shown in Fig. 7 the magnitude of the single-ion anisotropy at the tricritical point decreases as the value of  $R$  increases because the transverse fluctuations weaken

TABLE V. Estimates of  $\gamma$  for selected values of  $D/2Jz$ ;  $R = 0.25$ .

$D/2Jz$	$\gamma$
-0.466	1.00
-0.407	1.18
-0.310	1.21
-0.220	1.23
-0.107	1.24
0.251	1.25
1.02	1.25
2.39	1.25
4.06	1.25



TABLE VI. (Continued).

$b^5_{ijkl}$	i	j	k	l	$b^5_{ijkl}$	i	j	k	l	$b^5_{ijkl}$	i	j	k	l	$b^6_{ijkl}$	i	j	k	l
-184064.	3	1	3	1	-55744.	5	0	2	1	373248.	7	1	0	0	141888.	1	2	2	1
-625008.	3	1	3	2	-17040.	5	0	2	2	47616.	7	1	2	0	2432.	1	2	2	2
65952.	3	1	3	3	-144.	5	0	2	3	12096.	7	1	2	1	202176.	1	2	2	3
-137112.	3	1	3	4	-1008.	5	0	2	4	-32256.	7	1	3	0	37056.	1	2	2	4
-63328.	3	1	4	0	-12000.	5	0	3	0	96768.	7	1	3	1	123936.	1	2	2	5
-166640.	3	1	4	1	34880.	5	0	3	1	-72576.	7	1	3	2	-97984./15.	1	2	3	0
-628656.	3	1	4	2	267456.	5	0	3	2	-1232640.	7	2	0	0	69888.	1	2	3	1
-1087944.	3	1	4	3	-22080.	5	0	3	3	-7680.	7	2	2	0	184416.	1	2	3	2
-15768.	3	1	4	4	9240.	5	0	3	4	-5760.	7	2	2	1	511968.	1	2	3	3
47728.	3	1	5	0	-16800.	5	0	4	0	-92544.	9	0	0	0	-190800.	1	2	3	4
-221152.	3	1	5	1	84384.	5	0	4	1	-1920.	9	0	2	1	688992.	1	2	3	5
424944.	3	1	5	2	-99432.	5	0	4	2	578688.	9	1	0	0	-1926528./5.	1	2	4	0
-489984.	3	1	5	3	56520.	5	0	4	3	-105216.	11	0	0	0	-771400.	1	2	4	1
208704.	3	1	5	4	-720.	5	0	4	4					-2421136.	1	2	4	2	
-16896.	3	2	0	0	-280.	5	0	5	0					-5840232.	1	2	4	3	
-143040.	3	2	2	0	-2480.	5	0	5	1					-125112.	1	2	4	4	
-33504.	3	2	2	1	11640.	5	0	5	2					-6432108.	1	2	4	5	
-65184.	3	2	2	2	-13872.	5	0	5	3					170432./5.	1	2	5	0	
4176.	3	2	2	3	6450.	5	0	5	4					-294816.	1	2	5	1	
-3024.	3	2	2	4	-216576./5.	5	1	0	0					-1837696.	1	2	5	2	
-106144.	3	2	3	0	186784.	5	1	2	0					-5198496.	1	2	5	3	
695424.	3	2	3	1	96480.	5	1	2	1					-15439344.	1	2	5	4	
1650096.	3	2	3	2	38352.	5	1	2	2					-12305424.	1	2	5	5	
-43392.	3	2	3	3	2784.	5	1	2	3					5624752./15.	1	2	6	0	
143640.	3	2	3	4	-10272.	5	1	3	0					-363408.	1	2	6	1	
140000.	3	2	4	0	-115520.	5	1	3	1					7523228.	1	2	6	2	
331552.	3	2	4	1	-906624.	5	1	3	2					10861292.	1	2	6	3	
1231176.	3	2	4	2	27840.	5	1	3	3					69465102.	1	2	6	4	
1776432.	3	2	4	3	-12600.	5	1	3	4					176838480.	1	2	6	5	
13320.	3	2	4	4	30240.	5	1	4	0					64272.	1	3	0	0	
-47904.	3	2	5	0	-161568.	5	1	4	1					-3500224./5.	1	3	2	0	
209760.	3	2	5	1	206376.	5	1	4	2					-1388976.	1	3	2	1	
-442608.	3	2	5	2	-133968.	5	1	4	3					-88096.	1	3	2	2	
609408.	3	2	5	3	280.	5	1	5	0					-702912.	1	3	2	3	
-319140.	3	2	5	4	2480.	5	1	5	1					-61728.	1	3	2	4	
410016.	3	3	0	0	-11640.	5	1	5	2					-210924.	1	3	2	5	
-10624.	3	3	2	0	16080.	5	1	5	3					-1320256./15.	1	3	3	0	
-131904.	3	3	2	1	-9450.	5	1	5	4					-70144.	1	3	3	1	
19824.	3	3	2	2	-601920.	5	2	0	0					11360.	1	3	3	2	
-2016.	3	3	2	3	-124992.	5	2	2	0					-1181472.	1	3	3	3	
124896.	3	3	3	0	288.	5	2	2	1					387504.	1	3	3	4	
-1083264.	3	3	3	1	-12096.	5	2	2	2					-650304.	1	3	3	5	
-1520976.	3	3	3	2	-1296.	5	2	2	3					2083808.	1	3	4	0	
-17280.	3	3	3	3	-9984.	5	2	3	0					4011576.	1	3	4	1	
-37800.	3	3	3	4	370944.	5	2	3	1					11967856.	1	3	4	2	
-140064.	3	3	4	0	893376.	5	2	3	2					19878024.	1	3	4	3	
-212640.	3	3	4	1	-13440.	5	2	4	0					1280304.	1	3	4	4	
-1125528.	3	3	4	2	77184.	5	2	4	1					10279884.	1	3	4	5	
-1206288.	3	3	4	3	-115488.	5	2	4	2					-713024./5.	1	3	5	0	
16640.	3	3	5	0	84672.	5	2	4	3					1447392.	1	3	5	1	
-69600.	3	3	5	1	1249920.	5	3	0	0					5813440.	1	3	5	2	
156720.	3	3	5	2	-13056.	5	3	2	0					16671264.	1	3	5	3	
-256320.	3	3	5	3	-9792.	5	3	2	1					35012592.	1	3	5	4	
170100.	3	3	5	4	32256.	5	3	3	0					14700624.	1	3	5	5	
-556416.	3	4	0	0	-290304.	5	3	3	1					-3805552./3.	1	3	6	0	
87936.	3	4	2	0	-217728.	5	3	3	2					1033152.	1	3	6	1	
65952.	3	4	2	1	151296./5.	7	0	0	0					-22500908.	1	3	6	2	
-62208.	3	4	3	0	-39936.	7	0	2	0					-29741484.	1	3	6	3	
559872.	3	4	3	1	-14784.	7	0	2	1					-166694934.	1	3	6	4	
419904.	3	4	3	2	-2880.	7	0	2	2					-286983672.	1	3	6	5	
49536.	3	4	4	0	-432.	7	0	2	3					-327680.	1	4	0	0	
38016.	3	4	4	1	32256.	7	0	3	0					2521600.	1	4	2	0	
395280.	3	4	4	2	-96768.	7	0	3	1					3547200.	1	4	2	1	
272160.	3	4	4	3	57600.	7	0	3	2					245952.	1	4	2	2	
17600.	5	0	0	0	3600.	7	0	4	2					800928.	1	4	2	3	
-48736.	5	0	2	0	-2016.	7	0	4	3					69408.	1	4	2	4	













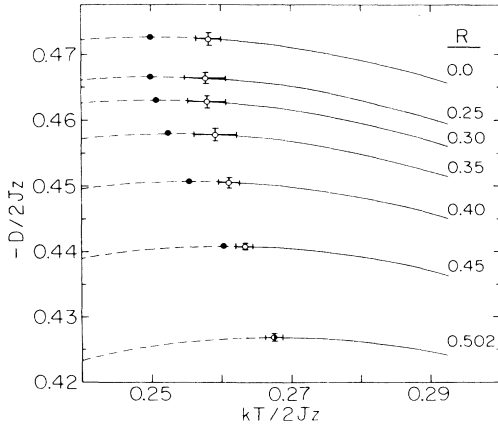


FIG. 7. Second-order phase boundaries for easy plane values of  $D$ ; fcc lattice. Open circles mark the tricritical points. Solid circles mark the peaks of the second-order boundaries. Dashed lines are metastable states in the first-order region.

the longitudinal ordering as does the easy-plane single-ion anisotropy. The temperature of the tricritical point is not so sensitive as  $R$  changes especially for the small values of  $R$ . On each curve of divergent susceptibility the point with the maximum value of  $D$  (the peak) is marked with a closed circle. As  $R$  increases, the distance between the peak and tricritical point becomes smaller and the two points eventually come together at  $R_c = 0.502 \pm 0.002$  ( $D/2Jz = 0.426 \pm 0.001$ ,  $kT/2Jz = 0.267 \pm 0.002$ ) where the uncertainty is assigned by taking the difference between the fifth- and sixth-order estimates. While the transverse ordered phase cannot be studied with the present series, the following argument suggests that for  $R$  greater than  $R_c$  a bicritical point appears in the phase diagram. The behavior near the bicritical point has been more extensively studied for the uniaxial antiferromagnet with an external field.<sup>27</sup> It is shown that the two second-order phase boundary lines meet tangentially with the first-order phase boundary line at the bicritical point, that is the three phase boundary lines have the same slope at the bicritical point. While the mean-field picture fails in showing such behavior, its qualitative features are presumably acceptable. It is observed that in the mean-field phase diagram of the currently studied model the first-order line separating the transverse and longitudinal ordered phases has a slight upward curvature and a positive slope at the bicritical point. For values of  $R$  less than  $R_c$  the slope of the phase boundary at the tricritical point remains negative. As  $R$  approaches  $R_c$  (MFT), which is 0.462, the congruence of the tricritical point and the critical endpoint produces a bicritical point. The behavior of the mean-field picture with the correc-

tion that the three phase boundary lines assume the same slope at the bicritical point leads to the conjecture that for  $R > 0.502$  a bicritical point appears in the phase diagram. The full picture of the phase diagram can only be obtained with the linked-cluster series including the transverse field and ordering.

#### IV. CONCLUSION

In this paper we have demonstrated the use of the multiple-site Wick reduction theorem to generate a linked-cluster series (to the sixth order) for a magnetic system with single-ion anisotropy and Heisenberg exchange interactions. The linked-cluster series reduces to the conventional high-temperature series in the disordered phase but can also be used to make accurate estimates of the physical quantities in the ordered phase. Thus tricritical points, first-order phase boundaries, temperature dependence of the magnetization and other properties can be studied. This is the first time a linked-cluster series in both ordered and disordered phases for a quantum spin system with a single-ion anisotropy has been generated and the tricritical phenomena can be studied. Experimental measurements of the transverse susceptibilities of the spin-1 easy-axis Heisenberg ferromagnets have shown the failure of the mean-field approximation in predicting the behavior.<sup>3</sup> In addition, it has been shown that the transverse fluctuations play the major role in the creation of a peak in the transverse susceptibility at the Curie temperature.<sup>13</sup> The extension of the current calculation to include the transverse ordering and transverse field will be of immediate interest.

#### ACKNOWLEDGMENTS

We acknowledge the Florida State Computer Center for providing the computer time on the Cyber 730 and 760 for the present calculation. We also acknowledge the helpful communication of H. H. Chen. This research was supported in part by the National Science Foundation under Grant No. DMR-8404954.

#### APPENDIX

The coefficients in the magnetization, susceptibility, and specific heat series are polynomials in the variables  $p$ ,  $q$ ,  $R$ , and  $(\beta D)^{-1}$  as

$$m_n = \sum_{i,j,k,l} b_{ijkl}^n p^i q^j R^k (\beta D)^{-l}, \quad (\text{A1})$$

$$a_n = \sum_{i,j,k,l} c_{ijkl}^n p^i q^j R^k (\beta D)^{-l}, \quad (\text{A2})$$

$$g_n = \sum_{i,j,k,l} d_{ijkl}^n p^i q^j R^k (\beta D)^{-l}. \quad (\text{A3})$$

The coefficients in Eqs. (A1)–(A3) are listed in Table VI for the fcc lattice series coefficients of the magnetization, paramagnetic susceptibility, and paramagnetic specific-heat series.

<sup>1</sup>R. B. Stinchcombe, G. Horwitz, F. Englert, and R. Brout, *Phys. Rev.* **130**, 155 (1963); R. B. Stinchcombe, *J. Phys. C* **6**, 2459 (1973); V. G. Vaks, A. I. Larkin, and S. A. Pikin, *Zh. Eksp. Teor. Fiz.* **53**, 1089 (1967) [*Sov. Phys.—JETP* **26**, 647

(1968)].

<sup>2</sup>R. Brout in *Magnetism IIA*, edited by G. T. Rado and H. Suhl (Academic, New York, 1965).

<sup>3</sup>R. M. Suter, M. Karnezos and S. A. Friedberg, *J. Appl. Phys.*

- 55, 2444 (1984).
- <sup>4</sup>G. S. Rushbrooke, G. A. Baker, and P. J. Wood, in *Phase Transitions and Critical Phenomena Vol. 3*, edited by C. Domb and M. S. Green (Academic, New York, 1974).
- <sup>5</sup>Y.-L. Wang, C. Wentworth, and B. Westwanski, *Phys. Rev. B* **32**, 1805 (1985); Y.-L. Wang and C. Wentworth, *J. Appl. Phys.* **57**, 3329 (1985).
- <sup>6</sup>M. Wortis, in *Phase Transitions and Critical Phenomena Vol. 3*, Ref. 4.
- <sup>7</sup>M. A. Moore, D. Jasnow, and M. Wortis, *Phys. Rev. Lett.* **22**, 940 (1969).
- <sup>8</sup>D. Jasnow and M. Wortis, *Phys. Rev.* **176**, 739 (1968).
- <sup>9</sup>Y.-L. Wang and F. Lee, *Phys. Rev. B* **29**, 5156 (1984).
- <sup>10</sup>Y.-L. Wang and F. Lee, *Phys. Rev. Lett.* **38**, 912 (1977).
- <sup>11</sup>K. Rauchwarger, S. Jafarey, and Y.-L. Wang, *Phys. Rev. B* **19**, 2712 (1979).
- <sup>12</sup>J. Johnson and Y.-L. Wang, *Phys. Rev. B* **24**, 5204 (1981).
- <sup>13</sup>C. Wentworth and Y.-L. Wang, *J. Phys. C* **18**, 3763 (1985).
- <sup>14</sup>A. L. Fetter and J. D. Walecka, *Quantum Theory of Many-Particle Systems* (McGraw-Hill, New York, 1971).
- <sup>15</sup>C. Domb and M. F. Sykes, *Phys. Rev.* **128**, 168 (1962).
- <sup>16</sup>G. Horwitz and H. Callen, *Phys. Rev.* **124**, 1757 (1961).
- <sup>17</sup>F. Lee and H. H. Chen, *Phys. Rev. B* **30**, 2724 (1984).
- <sup>18</sup>H. Strubbe, *Comp. Phys. Comm.* **8**, 1 (1974).
- <sup>19</sup>C. Wentworth, Ph.D. dissertation, Florida State University, 1986 (unpublished).
- <sup>20</sup>D. W. Wood and N. W. Dalton, *J. Phys. C* **5**, 1675 (1972).
- <sup>21</sup>D. C. Jou and H. H. Chen, *J. Phys. C* **6**, 2713 (1973).
- <sup>22</sup>M. R. H. Khajepour, Y.-L. Wang, and R. A. Kromhout, *Phys. Rev. B* **12**, 1849 (1975).
- <sup>23</sup>D. S. Gaunt and A. J. Guttman, in *Phase Transitions and Critical Phenomena Vol. 3*, Ref. 4.
- <sup>24</sup>G. A. Baker and P. Graves-Morris, *Padé Approximants* (Addison-Wesley, London, 1981).
- <sup>25</sup>D. S. Gaunt and G. A. Baker, *Phys. Rev. B* **1**, 1184 (1970).
- <sup>26</sup>J. Oitmaa, *J. Phys. C* **5**, 435 (1972).
- <sup>27</sup>J. M. Kosterlitz, D. R. Nelson, and M. E. Fisher, *Phys. Rev. B* **13**, 412 (1976).